

RESEARCH ARTICLE | MARCH 14 2022

Enhancing ultrasound transmission and focusing through a stiff plate with inversely optimized auxiliary meta-lens

He Gao; Zhongming Gu; Shanjun Liang; ... et. al

 Check for updates

Appl. Phys. Lett. 120, 111701 (2022)

<https://doi.org/10.1063/5.0085462>


View
Online


Export
Citation

CrossMark

Articles You May Be Interested In

A high-sensitivity and fast-response nanocomposites-inspired sensor for acousto-ultrasonics-based structural health monitoring

Proc. Mtgs. Acoust (December 2017)

Experimental verification of phased receiving waveguide array for ultrasonic imaging in aggressive liquids

Proc. Mtgs. Acoust (December 2017)



Time to get excited.
Lock-in Amplifiers – from DC to 8.5 GHz

[Find out more](#)

 Zurich
Instruments

Enhancing ultrasound transmission and focusing through a stiff plate with inversely optimized auxiliary meta-lens

Cite as: Appl. Phys. Lett. **120**, 111701 (2022); doi: [10.1063/5.0085462](https://doi.org/10.1063/5.0085462)

Submitted: 17 January 2022 · Accepted: 3 March 2022 ·

Published Online: 14 March 2022



View Online



Export Citation



CrossMark

He Gao,¹  Zhongming Gu,¹  Shanjun Liang,²  Tuo Liu,¹  Jie Zhu,^{3,a)}  and Zhongqing Su^{1,a)} 

AFFILIATIONS

¹Department of Mechanical Engineering, The Hong Kong Polytechnic University, Kowloon, Hong Kong

²Division of Science, Engineering and Health Studies, College of Professional and Continuing Education, Hong Kong Polytechnic University, Hung Hom, Kowloon, Hong Kong

³Institute of Acoustics, School of Physics Science and Engineering, Tongji University, Shanghai 200092, People's Republic of China

Note: This paper is part of the APL Special Collection on Acoustic and Elastic Metamaterials and Metasurfaces.

^{a)}Authors to whom correspondence should be addressed: jiezh@tongji.edu.cn and zhongqing.su@polyu.edu.hk

ABSTRACT

Effective sound energy transmission and beam manipulation through stiff and dense materials such as metal remain daunting tasks. It is in part attributable to the vast impedance mismatch between those materials and ambient media. Adding openings may facilitate to better bridge energy over, yet ineffective in many applications and may also damage the structural integrity. Here, we present an auxiliary ultrasound focusing meta-lens for stiff and dense materials. It offers significantly enhanced ultrasound transmission and focusing through a stiff metal plate yet without enforcing any through holes or openings. The simple, one-sided only meta-structures are designed and optimized by an inverse strategy based on the genetic algorithm. We numerically and experimentally demonstrate the much enhanced ultrasound transmission when the meta-lens is added to a flat brass plate, along with the capability to offer simultaneous ultrasound focusing. This design methodology can be easily extended to deal with more complex shaped target in a straightforward manner, offering a practical solution to the efficient tunneling of ultrasound energy through stiff and dense materials. With simple grating structures, the meta-lens can be easily fabricated, showing great application prospects in medical imaging and disease treatment.

Published under an exclusive license by AIP Publishing. <https://doi.org/10.1063/5.0085462>

Ultrasound has been widely exploited in numerous applications such as biomedical ultrasonography,^{1,2} particle manipulations,^{3,4} and nondestructive health monitoring.⁵ However, there is still a long way to go toward freewheeling control of ultrasound propagation and beam manipulation. Taking ultrasound focusing as an example, it has been a promising tool for noninvasive medical imaging and disease treatment. A variety of designs, including those that take advantage of latest phononic crystal and acoustic metamaterial development, were proposed to improve the focusing performance.^{6–19} Generally, for focusing of transmitted ultrasound with these meta-lenses,^{8–13} soft materials containing air scatters^{8,9} or structures with open channels^{10–13} are necessary to tune the refractive index distribution and boost the transmission efficiency. However, in many applications, ultrasound beams need to be transmitted through a stiff and dense layer with huge impedance mismatch, and without any openings (such as bones in soft tissues). They would inevitably experience

strong distortions and serious energy drop due to strong reflection and other effects caused by the dense material.

To improve the focusing performance of ultrasound transmitting through dense layers, complementary acoustic metamaterials have been proposed.^{8,20,21} However, the membrane-based meta-structures required for the negative and anisotropic properties usually are not sufficiently durable and may suffer from uncertain or changed prestress, which become issues in practical implementation.²⁰ Time-reversal based techniques have also been developed to introduce the holographic lenses with tailored phase patterns.^{15,22} However, they mainly aim at reconstructing the distorted transmitted field, but not the energy transmission improvement.

Here, we propose a three-dimensional ultrasound focusing enhancement (UFE) meta-lens with inverse design, which can increase the energy transmission and reduce the beam distortion for ultrasound focusing through a dense layer, simultaneously. The inverse

optimization is an emerging design approach that has shown powerful capabilities in acoustic devices development with various functionalities,^{23–28} such as acoustic cloak, beam splitter, and ventilation barrier. Here, our proposed inverse design methodology is genetic algorithm assisted. The structural parameters of the UFE meta-lens are the targeted variables to be globally optimized. The optimal UFE meta-lens has very simple structure and is made of the commonly used material (brass). When the UFE meta-lens is attached to a brass plate on one side, the transmitted power is remarkably enhanced and will be well focused, simultaneously, which can hardly be realized with conventional techniques. The performance of UFE meta-lens is experimentally demonstrated in a water tank, and the results are consistent with the numerical predictions.

Generally, the acoustic-solid interaction is neglected under some careful treatments in designing the underwater metamaterials,^{10,29–32} as it will greatly complicate the analytic solution. However here, we utilize the interaction of the lens with the background medium (water) to enhance the power transmission of the ultrasound beam. The inverse design method can be the most appropriate candidate to find the desired structure with the optimal performance numerically, avoiding the troublesome in theoretical calculations. It creates more possibilities to design functional metamaterial devices with irregular shapes or in complex environment.

First, we consider a system only containing a circular hard plate immersed in water, as illustrated in Fig. 1(a). This brass plate has a large impedance mismatch with the background medium (water), so that ultrasound waves incident on this plate will be almost totally reflected except for specific frequency components. We globally optimize a 3D axisymmetric lens to help the ultrasound beam to transmit through this hard plate. The lens is attached to the brass plate only on one side, as shown in Fig. 1(b), which does not need to damage

internal structure of the targeted object and, thus, is much closer to practical applications. With the lens, for the same incident beam, it can pass through the plate and is well focused behind the structure.

This UFE meta-lens is designed based on the inverse design method by optimizing its geometrical parameters. The inverse design concept combines the genetic algorithm with the finite element method. The inverse optimization target is to maximize the transmitted acoustic energy and rearrange the transmitted power through the hard plate to a specific position. The geometrical parameters of the UFE meta-lens are the optimization variables, which are initialized within a given range. Then, the genetic algorithm iteratively searches for the suitable values for these variables to gradually improve the score of the fitness function. In each cycle, these optimized values will be passed to the COMSOL Multiphysics for numerical calculations, and the calculated acoustic intensity profiles are then returned to the genetic algorithm to act as the fitness function. This process would be repeated until it satisfies the stopping criterion. Once the optimization process ends, the best fit values for the target variables would be output, and thus, the optimal structure can be obtained, as illustrated in Fig. 1(b).

The profile of one unit cell in the patterned stiff plate is presented in Fig. 1(c). Each unit cell is a circular ring with a part being removed, which is attached to the brass plate (height $h_0 = 1.8$ mm and radius $r = 65$ mm). The width and height of the base ring are $w_{i,1}$ and $h_{i,1}$ ($i = 1, 2, \dots, 9, 10$ is the number of the unit cell), respectively. A thinner and shorter ring (width is $w_{i,2}$ and height is $h_{i,2}$) is cut from the top side of the base ring to introduce more degrees of freedom. The shape of this selected ring structure can facilitate the experimental fabrication. The UFE meta-lens is composed of ten ring structures, which is periodically arranged along the radial direction of the hard plate (the period $p = 5$ mm), as demonstrated in Fig. 1(d). To leave some space for conveniently holding the sample in the measurements, the radius of the hard plate is designed to be larger than that of the AFE lens. The structural parameters of all the ring elements are the variables to be optimized, and the optimized results are given in Table I.

All the simulations in the optimization procedure are conducted with acoustic-solid interaction module in COMSOL Multiphysics.³³ The density and sound speed of water in pressure acoustics module are set to be 998 kg/m^3 and 1480 m/s , respectively. The density, Poisson's ration, and Young's modulus of brass in solid mechanics module are set to be 8960 kg/m^3 , 0.35 , and 110 GPa , respectively. The impedance ratio of brass (its sound speed is around 4400 m/s) to water is around 26.7 . This large impedance mismatch would inevitably block the incident wave to pass through the brass plate, as can be observed from Fig. 2(a), which shows the simulated intensity field for the stiff plate immersed in water. The incident plane wave is along the x direction, and then most of the energy is reflected. However, when the brass

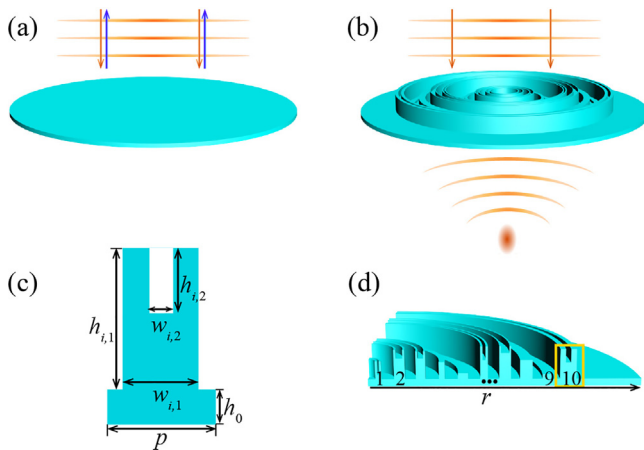


FIG. 1. Schematic of the UFE meta-lens. (a) and (b) Illustration of the ultrasound wave incident on the stiff plate and the stiff plate patterned with the optimized UFE meta-lens from the top side, respectively. The red and blue arrows illustrate the incident and reflected sound waves, respectively. (c) Profile of one unit cell in the patterned plate, encircled by the yellow box in (d). The total width of each cell p is set to be 5 mm. The other geometrical parameters are the targeted optimization variables. The height h_0 for the stiff plate is set to be 1.8 mm. (d) A quarter of the plate patterned with the UFE meta-lens. The lens is composed of ten ring structures. The radius of the stiff plate is set to be 65 mm.

TABLE I. The optimized geometric parameters of the AFE lens.

i	1	2	3	4	5	6	7	8	9	10
$w_{i,1}$ (mm)	1.5	2.6	2.3	1.4	2.4	1.8	2.8	3	2.2	3.9
$h_{i,1}$ (mm)	4.4	7.1	6.7	4.1	1.4	7.9	8	4.6	1.1	7.2
$w_{i,2}$ (mm)	0.4	1.6	1.3	0	0	0.7	2	0	0	1.2
$h_{i,2}$ (mm)	3.4	2.1	1.7	0	0	3.3	1.7	0	0	3.3

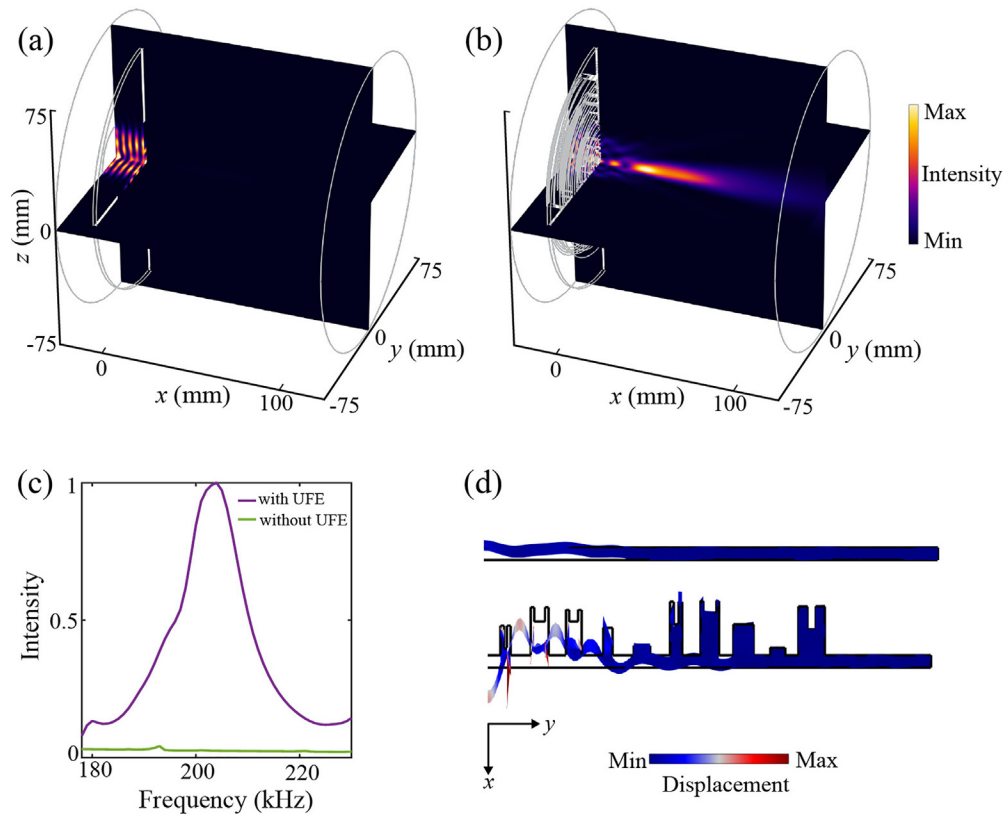


FIG. 2. Simulations for the plate with and without UFE meta-lens. (a) and (b) Simulated acoustic intensity fields for the bare plate and the plate patterned with the optimized UFE meta-lens, respectively. The frequency of the incident wave is 207 kHz. (c) The numerically calculated transmitted power as a function of frequency. The purple line and green line present the results for the plate with and without UFE meta-lens, respectively. (d) Radial profiles of the total displacements for the two structures. The upper panel is for the bare plate, and the lower panel is for the patterned plate. The color and deformation both denote the magnitude of the displacement.

plate is patterned with the optimized UFE meta-lens, the transmitted energy will be greatly enhanced and well focused, as shown in Fig. 2(b).

To further explore the enhancing performance of the lens, we numerically calculate the transmitted energy for the patterned plate at different frequencies. The according spectra of the transmitted power are presented in Fig. 2(c) in which the purple line and green line represent the results for the plate with and without UFE meta-lens, respectively. We can see that the UFE meta-lens can greatly improve the power transmission of the hard plate within a certain frequency range. The incident frequency for Figs. 2(a) and 2(b) is chosen to be 207 kHz, which is around the peak in the spectrum of the patterned plate [Fig. 2(c)]. In addition to the simulated acoustic fields in Figs. 2(a) and 2(b), we also examine and compare the total displacement fields in the bare plate and the patterned plate, as shown in Fig. 2(d). The diameter of the incident plane wave is chosen to be 38 mm to mimic the practical incident source, so that only the middle part of the structure is vibrating. It can be clearly seen that the displacement in the middle part of the plate with UFE meta-lens is much higher than that of the bare plate. Owing to the acoustic-solid interaction, the intrinsic modes of the plate patterned with the UFE meta-lens can be excited. The patterned plate has a larger vibrating displacement, which contributes to enhancing the transmitted sound energy through the stiff plate. Both the amplitude and phase responses of

the symmetric UFE meta-lens are optimized, so that the transmitted sound power can be well redistributed to the focusing spot.^{34–40}

Furthermore, we experimentally confirm the effectiveness of the UFE meta-lens. The uniform plate and the plate with the UFE meta-lens are fabricated via precision computerised numerical control (CNC) machining, with the manufacturing error being 0.1 mm. The inset of Fig. 3(a) is the photo of the brass plate patterned with the UFE meta-lens, whose material parameters keep consistent with the simulations. The according experiments are performed in UMS3 scanning tank with a 3D moving stage. During the measurements, the experimental sample is immersed in water and is held vertically with a clamp, as depicted in Fig. 3(a). The incident wave is excited by a tone burst signal with a frequency of 207 kHz, which is generated by the function/waveform generator (Keysight, Type 33210A) and transfers to the planar transducer (Precision Acoustics, Type TX_0.5_44). The signal transmitted through the sample is acquired with a needle hydrophone (Precision Acoustics, Type NH2000) and is then sent to and recorded by the mixed domain oscilloscope (Tektronix, Type MDO3014). The whole acoustic fields are obtained by moving the scanning platform in the specific plane with a step of 3 mm.

The measured transmitted acoustic intensity fields for the brass plate without and with UFE meta-lens are shown in Figs. 3(c) and 3(d),

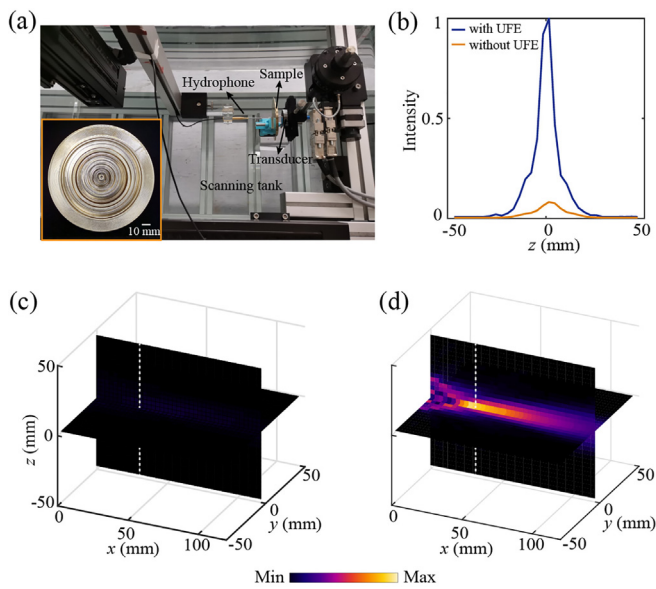


FIG. 3. Experimental setup and measured intensity fields. (a) The experimental setup in the UMS3 scanning tank. The inset in the yellow box is the photo of the brass plate patterned with optimized UFE meta-lens. (b) The intensity plots along the white dashed lines in (c) (yellow line) and (d) (blue line). (c) and (d) The measured acoustic intensity profiles for the plate without and with UFE meta-lens, respectively.

respectively. Here, the acoustic fields in the xy plane and xz plane are, respectively, measured. By comparing these two cases in Figs. 3(c) and 3(d), we can observe an obvious focal spot for the patterned plate with greatly enhanced intensity. To quantitatively see the transmission enhancement of the UFE meta-lens, the intensity profiles along the white dashed lines in Figs. 3(c) and 3(d) are calculated, respectively, as presented in Fig. 3(b). The intensity for the patterned plate (blue line) is more than ten times the result for the baseplate (yellow line), which confirms the focusing enhancement of the optimized lens.

Very interestingly, even though the optimized UFE meta-lens is designed to work at a specific frequency, it can practically enhance the ultrasound focusing within a certain frequency range, as predicted in Fig. 2(c). Here, we measure the intensity profiles of the patterned plate at different frequencies. The according results are given in Figs. 4(a) and 4(b), of which the frequencies of the incident ultrasound wave are selected to be 200 and 212 kHz, respectively. In these two cases, the transmitted sound fields still form a clear focal spot. We plot the intensity profiles along the propagation direction, as depicted in Fig. 4(c), which clearly show the hallmark of acoustic focusing. Also, the intensity profiles along the white dashed lines in these two cases are plotted in Fig. 4(d). An obvious peak appears at these two frequencies, and the intensities are slightly lower than that in Fig. 3(b). Actually, within this frequency range, the total displacement for the patterned plate is higher than that for the bare plate, which accounts for the fact that the optimized UFE meta-lens is robust to the incident frequency. This relatively broadband property possesses critical importance in many practical applications. In addition, the working bandwidth of the AFE lens is likely to be broadened by changing the shape of the unit cell to have more freedoms and variables in the optimization.

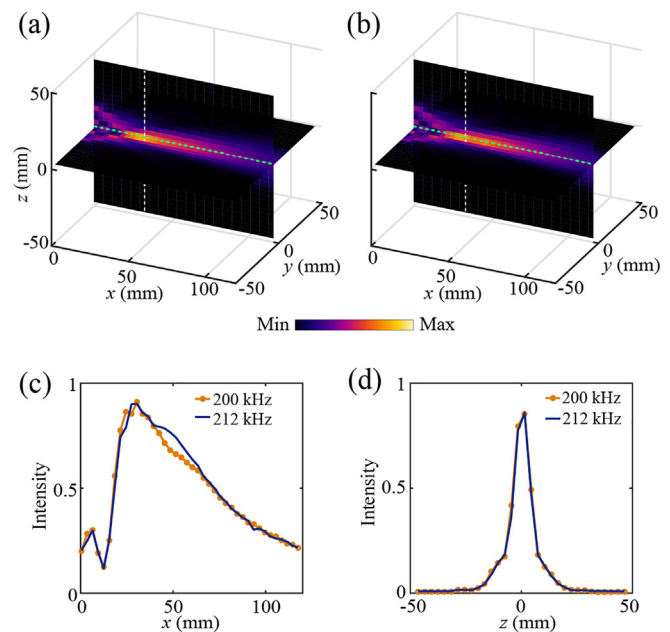


FIG. 4. The measured UFE at different frequencies. (a) and (b) The experimental results for the plate patterned with the UFE meta-lens with the incident frequency being 200 and 212 kHz, respectively. (c) and (d) The measured intensity profiles along the green dashed line and white dashed line, respectively. The blue line (solid line) and the yellow line (circle line) denote the results in (a) and (b), respectively.

In summary, we have proposed an inverse design scheme to fabricate a metamaterial lens that can realize ultrasound focusing and power transmission enhancement through a stiff plate without any openings, simultaneously. The UFE meta-lens is optimized by combining the genetic algorithm with the finite element method, which is numerically and experimentally demonstrated. This focusing enhancement is achieved by fully utilizing the acoustic-solid interaction, which is usually not considered in most of the underwater metamaterial designs. Moreover, the UFE meta-lens is of simple structures that can be easily manufactured, with a wide variety of available base materials (preferable with low internal damping) not limited to brass here, thereby showing great advantages in practical applications. This inverse design method is also applicable for the hard plate with any other materials or shapes. Thus, we envision that this optimization method opens more possibilities to design underwater acoustic devices with colorful functionalities, as this optimization method can greatly simplify the design procedure.

We wish to acknowledge the support from the Research Grants Council of Hong Kong SAR (Grant Nos. 15205219, C6013-18G, and AoE/P-502/20) and the National Natural Science Foundation of China (Grant No. 11774297).

AUTHOR DECLARATIONS

Conflict of Interest

The authors have no conflicts of interest to disclose.

DATA AVAILABILITY

The data that support the findings of this study are available from the corresponding authors upon reasonable request.

REFERENCES

- ¹C. Demene, J. Baranger, M. Bernal, C. Delanoe, S. Auvin, V. Biran, M. Alison, J. Mairesse, E. Harribaud, M. Pernot *et al.*, *Sci. Transl. Med.* **9**, eaah6756 (2017).
- ²C. Rabut, M. Correia, V. Finel, S. Pezet, M. Pernot, T. Deffieux, and M. Tanter, *Nat. Methods* **16**, 994 (2019).
- ³J. Li, C. Shen, T. J. Huang, and S. A. Cummer, *Sci. Adv.* **7**, eabi5502 (2021).
- ⁴Y. Yang, T. Ma, S. Li, Q. Zhang, J. Huang, Y. Liu, J. Zhuang, Y. Li, X. Du, L. Niu *et al.*, *Research* **2021**, 9781394.
- ⁵H. Selim, M. Delgado-Prieto, J. Trull, R. Pico, L. Romeral, and C. Cojocar, *Ultrasonics* **101**, 106000 (2020).
- ⁶X. Xia, Y. Li, F. Cai, H. Zhou, T. Ma, and H. Zheng, *Appl. Phys. Lett.* **117**, 021904 (2020).
- ⁷Y. Shen, X. Zhu, F. Cai, T. Ma, F. Li, X. Xia, Y. Li, C. Wang, and H. Zheng, *Phys. Rev. Appl.* **11**, 034009 (2019).
- ⁸A. Allam, K. Sabra, and A. Erturk, *Phys. Rev. Appl.* **13**, 064064 (2020).
- ⁹Z. Li, S. Yang, D. Wang, H. Shan, D. Chen, C. Fei, M. Xiao, and Y. Yang, *Appl. Phys. Lett.* **119**, 073501 (2021).
- ¹⁰Y. Ruan, X. Liang, Z. Wang, T. Wang, Y. Deng, F. Qu, and J. Zhang, *Appl. Phys. Lett.* **114**, 081908 (2019).
- ¹¹X. Su, A. N. Norris, C. W. Cushing, M. R. Haberman, and P. S. Wilson, *J. Acoust. Soc. Am.* **141**, 4408 (2017).
- ¹²J. Chen, J. Xiao, D. Lisevych, A. Shakouri, and Z. Fan, *Nat. Commun.* **9**, 4920 (2018).
- ¹³J. Chen, J. Rao, D. Lisevych, and Z. Fan, *Appl. Phys. Lett.* **114**, 104101 (2019).
- ¹⁴J. He, X. Jiang, H. Zhao, C. Zhang, Y. Zheng, C. Liu, and D. Ta, *Phys. Rev. Appl.* **16**, 024006 (2021).
- ¹⁵S. Jiménez-Gambín, N. Jiménez, J. M. Benlloch, and F. Camarena, *Phys. Rev. Appl.* **12**, 014016 (2019).
- ¹⁶S. Jiménez-Gambín, N. Jiménez, and F. Camarena, *Phys. Rev. Appl.* **14**, 054070 (2020).
- ¹⁷V. Chaplin, M. A. Phipps, and C. F. Caskey, *Phys. Med. Biol.* **63**, 105016 (2018).
- ¹⁸W. Legon, T. F. Sato, A. Opitz, J. Mueller, A. Barbour, A. Williams, and W. J. Tyler, *Nat. Neurosci.* **17**, 322 (2014).
- ¹⁹W. J. Elias, N. Lipsman, W. G. Ondo, P. Ghanouni, Y. G. Kim, W. Lee, M. Schwartz, K. Hynynen, A. M. Lozano, B. B. Shah *et al.*, *N. Engl. J. Med.* **375**, 730 (2016).
- ²⁰C. Shen, J. Xu, N. X. Fang, and Y. Jing, *Phys. Rev. X* **4**, 041033 (2014).
- ²¹J. Wang, F. Allein, N. Boechler, J. Friend, and O. Vazquez-Mena, *Phys. Rev. Appl.* **15**, 024025 (2021).
- ²²M. Ferri, J. M. Bravo, J. Redondo, and J. V. Sánchez-Pérez, *Ultrasound Med. Biol.* **45**, 867 (2019).
- ²³L. Sanchis, V. M. García-Chocano, R. Llopis-Pontiveros, A. Climente, J. Martínez-Pastor, F. Cervera, and J. Sánchez-Dehesa, *Phys. Rev. Lett.* **110**, 124301 (2013).
- ²⁴L. Fan and J. Mei, *Phys. Rev. Appl.* **14**, 044003 (2020).
- ²⁵W. W. Ahmed, M. Farhat, X. Zhang, and Y. Wu, *Phys. Rev. Res.* **3**, 013142 (2021).
- ²⁶Y.-T. Luo, P.-Q. Li, D.-T. Li, Y.-G. Peng, Z.-G. Geng, S.-H. Xie, Y. Li, A. Alù, J. Zhu, and X.-F. Zhu, *Research* **2020**, 8757403.
- ²⁷J. Weng, Y. Ding, C. Hu, X.-F. Zhu, B. Liang, J. Yang, and J. Cheng, *Nat. Commun.* **11**, 6309 (2020).
- ²⁸Z.-X. Xu, H. Gao, Y.-J. Ding, J. Yang, B. Liang, and J.-C. Cheng, *Phys. Rev. Appl.* **14**, 054016 (2020).
- ²⁹Y. Chen, M. Zheng, X. Liu, Y. Bi, Z. Sun, P. Xiang, J. Yang, and G. Hu, *Phys. Rev. B* **95**, 180104 (2017).
- ³⁰Z. Sun, X. Sun, H. Jia, Y. Bi, and J. Yang, *Appl. Phys. Lett.* **114**, 094101 (2019).
- ³¹Y. Bi, H. Jia, Z. Sun, Y. Yang, H. Zhao, and J. Yang, *Appl. Phys. Lett.* **112**, 223502 (2018).
- ³²L.-S. Zeng, Y.-X. Shen, X.-S. Fang, Y. Li, and X.-F. Zhu, *Ultrasonics* **117**, 106548 (2021).
- ³³D. G. Gorman, J. Reese, J. Horacek, and K. Dedouch, *Proc. Inst. Mech. Eng., Part C* **215**, 1303 (2001).
- ³⁴Z. He, H. Jia, C. Qiu, S. Peng, X. Mei, F. Cai, P. Peng, M. Ke, and Z. Liu, *Phys. Rev. Lett.* **105**, 074301 (2010).
- ³⁵H. Jia, M. Ke, C. Li, C. Qiu, and Z. Liu, *Appl. Phys. Lett.* **102**, 153508 (2013).
- ³⁶C. Li, M. Ke, Y. Ye, S. Xu, C. Qiu, and Z. Liu, *Appl. Phys. Lett.* **105**, 023511 (2014).
- ³⁷Y. Li, B. Liang, X. Zou, and J. Cheng, *Chin. Phys. Lett.* **29**, 114301 (2012).
- ³⁸F. Cai, Z. He, Z. Liu, L. Meng, X. Cheng, and H. Zheng, *Appl. Phys. Lett.* **99**, 253505 (2011).
- ³⁹R. Hao, C. Qiu, Y. Ye, C. Li, H. Jia, M. Ke, and Z. Liu, *Appl. Phys. Lett.* **101**, 021910 (2012).
- ⁴⁰J.-P. Xia and H.-X. Sun, *Appl. Phys. Lett.* **106**, 063505 (2015).